
COBias and Debias: Balancing Class Accuracies for Language Models in Inference Time via Nonlinear Integer Programming

Ruixi Lin Yang You

Department of Computer Science
National University of Singapore
`{ruixi,youy}@comp.nus.edu.sg`

Abstract

Large language models (LLMs) are good knowledge bases but struggle to perform equally well for all classes in text classification tasks. This paper investigates a fundamental inference-time problem in language models: imbalanced class accuracies. We find what's underneath the issue is a tendency to over-predict some classes while under-predicting some others. This class accuracy imbalance is difficult to solve from the root via better pre-training or fine-tuning strategies, but we show it can be effectively mitigated via inference-time combinatorial optimization. To this end, we conceptualize and quantify the over- and under-prediction issue as the Contextual Oddity Bias (COBias), and propose the Debiasing as Nonlinear Integer Programming (DNIP) model to correct in-context learned class probabilities based on minimizing COBias and maximizing overall accuracy, without LLM parameter update. Considering that the DNIP model implicitly contains non-differentiable elements, we therefore use the simulated annealing algorithm to solve it. Extensive evaluations on three LLMs across seven NLP classification tasks in different prompting settings show that DNIP simultaneously achieves significant COBias reduction (-27%) and accuracy improvement (+12%) over the conventional ICL approach, suggesting that inference-time mitigation of class accuracy imbalance is a promising direction to push forward LLM performances.

1 Introduction

The fact that large language models (LLMs) achieve remarkable overall test accuracy by few-shot in-context learning (ICL) [1] can obscure a large difference in individual class accuracies. Mitigating class accuracy imbalance is under-explored, but important to facilitate a smoother user experience and reduce safety risks.

It could be difficult to disentangle all the factors that cause class accuracy imbalance. Resolving the issue from the root through pre-training or fine-tuning, leveraging data selection or data augmentation, is neither easy nor cost-effective. To overcome the issue, we conceptualize a bias metric, the Contextual Oddity Bias (COBias; Section 2), to quantify class accuracy imbalance from inference-time over-predictions and under-predictions. We aim to reduce COBias by directly rectifying the in-context learned LLM output class probabilities. We propose DNIP, the Debiasing as Nonlinear Integer Programming model, to search for correction weights leveraging combinatorial optimization, without updating LLM parameters (Section 3). These weights adjust class probabilities towards lower COBias and higher overall accuracy. On three widely used different-scale LLMs across seven NLP evaluation datasets, and in different ICL settings, we show the effectiveness of DNIP.

Our key messages are as follows:

- We introduce the COBias evaluation metric to quantify the class accuracy imbalance in language model predictions, where LLMs of different scales and families consistently exhibit a large COBias score.
- We propose Debiasing as Nonlinear Integer Programming (DNIP) method to find class correction weights to correct ICL output class probabilities, which minimize COBias and maximize accuracy. An efficient simulated annealing algorithm is adopted to solve the nonlinear integer programming model.
- DNIP achieves the best of both worlds of lower COBias and higher overall accuracy. For example, on Llama-2-13B, DNIP significantly reduces COBias (avg. 40.5% \rightarrow 14.3%) and improves overall accuracy (avg. 59.4% \rightarrow 69.2%) over the 1-shot ICL results, and it reduces COBias even further over the 5-shot ICL results (avg. 39.2% \rightarrow 10.3%).

2 Over-prediction, Under-prediction, and the Contextual Oddity Bias

	Pred.						
	World	Sports	Business	Tech	All	Acc.	
<i>True</i>	World	1093	64	126	3	1286	0.85
	Sports	9	1247	14	0	1270	0.98
	Business	25	4	1167	8	1204	0.97
	Tech	156	27	822	235	1240	0.19
	All	1283	1342	2129	246	5000	-
Prec.		0.85	0.93	0.55	0.96	-	-

Table 1: Over-prediction in class *Business* and under-prediction in class *Tech* in Llama-2-13B, shown by the test confusion matrix for AGNews.

	Pred.						
	World	Sports	Business	Tech	All	Acc.	
<i>True</i>	World	1100	50	67	69	1286	0.86
	Sports	16	1240	11	3	1270	0.98
	Business	44	2	1028	130	1204	0.85
	Tech	55	7	138	1040	1240	0.84
	All	1215	1299	1244	1242	5000	-
Prec.		0.91	0.95	0.83	0.84	-	-

Table 2: Significantly improved test accuracy of the under-predicted class *Tech* for AGNews after DNIP correction.

Over-predictions and under-predictions can hurt LLM prediction capabilities. To see how, Table 1 presents an example of observed over-predictions and under-predictions in Llama-2-13B. We prompt the LLM on the AGNews news classification [2], and find that Llama-2-13B greatly over-predicts *Business* while under-predicting *Tech*, leading to low accuracy in *Tech* (19%). Over-/Under-prediction happens in many downstream tasks and also in larger models such as ChatGPT (Appendix A), suggesting room for improvements so that LLMs can predict all classes with equally good accuracy.

Conceptualizing Over-prediction and Under-prediction into the Contextual Oddity Bias. To introduce the Contextual Oddity Bias, we first elaborate the over-/under-prediction observations. In Table 1, the most significant contributor to the under-prediction in *Tech* (accuracy: 19%) is the 822 ground-truth *Tech* instances which are wrongly predicted as *Business*¹. That is, the output class *Business* which a ground-truth class *Tech* is most wrongly predicted as can reflect the model’s inference bias towards an output class for the given ground-truth class. To precisely quantify this inference bias, we first conceptualize *odd* classes. An odd class is an output class which holds the most wrong predictions of a ground-truth class. That is, there is always an odd class to a ground-truth class. For N classes and M instances, let y and \hat{y} denote the ground-truth class and the prediction respectively, let u_{c_i, c_j} denote the number of ground-truth c_i instances that are wrongly predicted as c_j ,

$$u_{c_i, c_j} = \sum_m \mathbb{1}\{y_m = i, \hat{y}_m = j\}, \quad (1)$$

$$\text{odd}_i = \text{odd_class}(c_i) := \arg \max_{c_j} u_{c_i, c_j}, \quad (2)$$

where $m = 1, \dots, M, i, j = 1, \dots, N, j \neq i$, $\mathbb{1}\{\cdot\} = 1$ if the condition holds and 0 otherwise. For example, $\text{odd_class}(\text{Tech}) = \text{Business}$. Then, we propose to quantify how much an odd class contributes to under-predicting a ground-truth class. One may immediately use the ratio of the number of odd class predictions over that of the ground-truth instances, e.g., use 822/1240 to measure the odd *Business*’s “hurt” to the ground-truth *Tech*, but minimizing these rates alone may not adequately

¹It simultaneously leads to a fairly low precision score of 55% in *Business*. In fact, the low precision score in *Business* and the low recall/accuracy score in *Technology* co-reflect each other. In other words, class accuracies are essential indicators for class performances. All current evaluation metrics are computed by Python scikit-learn. Note that by scikit-learn, class recall is the same as class accuracy.

mitigating class accuracy imbalances (More analyses on this measurement are in Appendix B.). A simpler yet better measurement is the absolute accuracy difference between the odd class and the ground-truth class. For example, the 78% difference between *Business* (97%) and *Tech* (19%) quantifies how much *Tech* is under-predicted. The 19% also implicitly reflects the 822 wrong predictions in *Business*. It is noted that these accuracy differences sometimes fail to capture the *ground-truth-and-odd* relationships. For instance, *World* is the odd class to *Business*, but the former is 12% (97%-85%) below the latter. Despite the drawback, minimizing these differences will in return significantly reduce odd class predictions and improve under-predicted classes' accuracies.

The Contextual Oddity Bias. To this end, we propose Contextual Oddity Bias (COBias). First, we propose COBias_{single}, the absolute value of the accuracy difference between a ground-truth class and its odd class. Formally, given an N classes and M instances, let x_m denote an instance whose label is y_m . After obtaining few-shot prompted softmax probabilities over the vocabulary at the output position, we take the probabilities for the class tokens and normalize them to form class probabilities, i.e., $\mathbf{p}_m = (p_{m1}, \dots, p_{mN})$ is the normalized class probabilities for classes c_1, \dots, c_N . Then the prediction \hat{y}_m is $\arg \max_{j \in \{1, \dots, N\}} \mathbf{p}_m$. For a given class c_i , let A_{odd_i} and A_{c_i} denote the accuracies for the odd class odd_i and c_i respectively, the COBias_{single} metric is computed as:

$$\text{COBias}_{\text{single}} = \frac{1}{N} \sum_i \left| A_{\text{odd}_i} - A_{c_i} \right|, \quad (3)$$

where class accuracy $A_{c_i} = \frac{1}{|\mathcal{S}_{c_i}|} \sum_{m \in \mathcal{S}_{c_i}} \mathbb{1}\{\hat{y}_m = y_m\}$, \mathcal{S}_{c_i} is the set of indices for class c_i instances. Similarly, $A_{\text{odd}_i} = \frac{1}{|\mathcal{S}_{\text{odd}_i}|} \sum_{m \in \mathcal{S}_{\text{odd}_i}} \mathbb{1}\{\hat{y}_m = y_m\}$, where $\mathcal{S}_{\text{odd}_i}$ is the set of indices for class odd_i instances. COBias_{single} measures a model's tendency to under-predict the true answer and mostly mistake it as an odd answer. The odd classes in a same downstream task can vary across different models. That's why we use "contextual" to mean that the oddity of an answer depends on the model or task.

Beyond the single odd classes, there could also be a secondly most-, or third most-, to the least-frequent wrongly predicted class, i.e., the odd, the second odd, to the least odd classes. For example, for ground-truth *Tech*, *Business* is the odd, while *World* is the second odd, and *Sports* is the least odd. We extend COBias_{single} to every pair of classes. This arrives at the ultimate **the COBias metric** as follows.

$$\text{COBias} = \binom{N}{2}^{-1} \sum_{i=1}^{N-1} \sum_{j=i+1}^N \left| A_{c_i} - A_{c_j} \right|. \quad (4)$$

COBias directly reflects the inter-class imbalance in accuracy. Although the absolute value of accuracy differences of some pairs in Equation 4 may mask the odd class, it reflects a well-rounded measurement and a powerful metric when minimal class accuracy imbalance is demanded.

3 Improving LLM Outputs by *Debiasing as Nonlinear Integer Programming*

Essentially, we aim to rectify biased few-shot prompted LLM class probabilities with correction weights, so that corrected class probabilities should lead to less class accuracy imbalance. With this goal, we propose an inference-time nonlinear integer programming (NIP) selection model to search for optimal correction weights from a weight scale that directly minimizes COBias while maximizing overall accuracy. Therefore, the correction weights are optimized by the NIP model on a set of given LLM output class probabilities with ground-truth labels. For a test instance, after obtaining its class probabilities, the learned correction weights are applied to correct them. An overview of the proposed Debiasing as Nonlinear Integer Programming (DNIP) method is shown in Figure 1.

3.1 The DNIP Objective

We first introduce a discrete K -point correction weight scale ω to select correction weights from. We denote $\omega = (\omega_1, \dots, \omega_K)$, and $\omega_k = k/K$ is a value from the scale. For example, a 10-point scale renders $\omega = (0.1, \dots, 1.0)$. To debias the N -dimensional \mathbf{p}_m , for each class j , $\mathbf{p}_{m,j}$ multiplies a correction weight selected from ω to obtain a corrected class probability.

Therefore, finding optimal correction weights for all N classes becomes a combinatorial optimization problem: each class selects a weight from the K -point scale, so we need to find the optimal

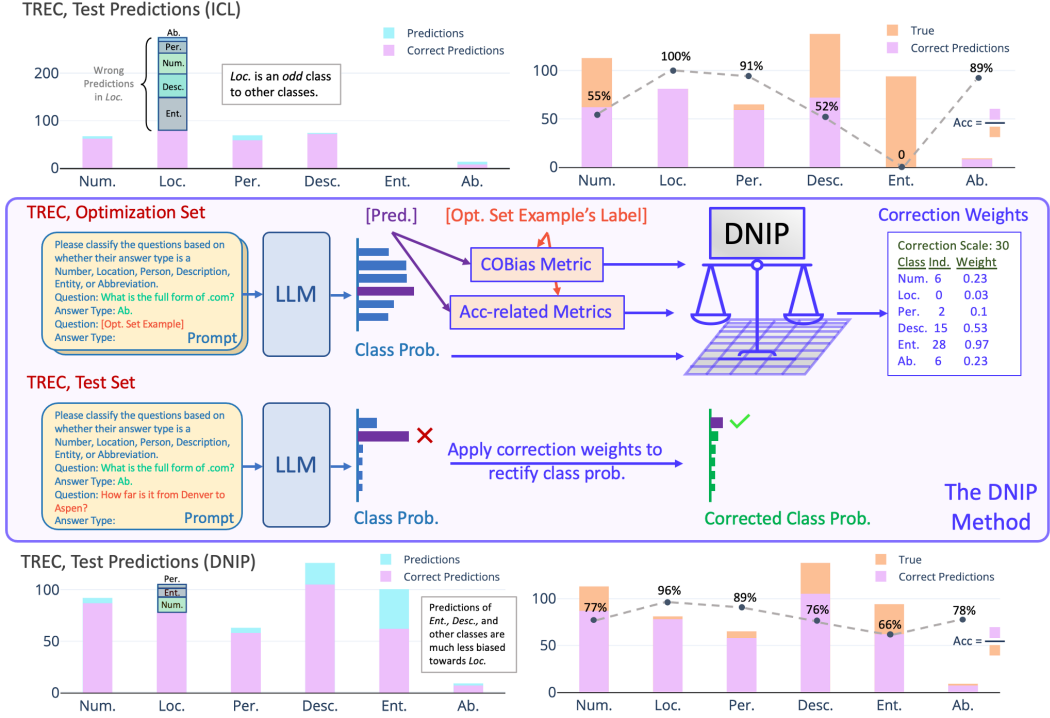


Figure 1: An overview of the DNIP method. We take the TREC [3] task for illustration; the ICL approach uses 1-shot prompting whose prompt is given by light yellow text boxes. The upper-left plot shows that *Loc.* is an odd class to the others, holding their majority wrong predictions, especially for *Ent.*; the upper-right plot demonstrates the stark contrast in class accuracy, with 100% for *Loc.* and 0 for *Ent.*. The bottom plots show that DNIP greatly reduces pairwise class accuracy differences, especially boosting accuracy for *Ent.* (0 → 66%).

combination of the selections. To this end, we formulate the following correction weight selection model towards minimizing pairwise class accuracy differences and maximizing overall accuracy. Formally, we define integer selection variables $\xi = (\xi_1, \dots, \xi_N)$ that selects a weight index k for the n -th class probability in \mathbf{p}_m , namely, $\xi_n = k$ if the n -th class selects ω_k . As a result, the DNIP model can be given by:

$$\min \quad Z(\xi) = \frac{1}{M} \sum_{m=1}^M \mathbb{1}\{\hat{y}_m \neq y_m\} + \beta \binom{N}{2}^{-1} \sum_{i=1}^{N-1} \sum_{j=i+1}^N \left| A_{c_i} - A_{c_j} \right| - \tau \sum_{j=1}^N \text{PMI}_j \quad (5)$$

$$\text{s.t.} \quad \hat{y}_m = \arg \max_{n \in \{1, \dots, N\}} \omega_{\xi_n} p_{mn}, \quad m = 1, \dots, M \quad (6)$$

$$\text{PMI}_j = \text{PMI}(\hat{S}^j, S^j) = \log \frac{f(\hat{S}^j, S^j)}{f(\hat{S}^j)f(S^j)}, \quad j = 1, \dots, N \quad (7)$$

$$\xi_n \in \{1, \dots, K\}, \quad n = 1, \dots, N \quad (8)$$

where β and τ are parameters that control the bias and the PMI terms respectively. The PMI term is introduced to maximize the pointwise mutual information between ground-truth class j instances and predicted class j , which can be seen as a confidence level, or a constraint to penalize each individual class. \hat{S}^j and S^j denote the instances of prediction j and true label j respectively, $f(\hat{S}^j)$ is the ratio between the number of instances with prediction j and the total number of instances, similarly, $f(S^j)$ is the ratio between the number of instances labeled j and the total number of instances, $f(\hat{S}^j, S^j)$

is the ratio between the number of correct predictions of class j and the total number of instances. In actual computations, we apply add- μ smoothing to the respective ratios in the numerator and denominator to smooth out zeros. The smoothing coefficient μ is selected along other parameters on a development set.

Intuitively, the first term directly minimizes error rates, the second term COBias directly minimize the inter-class accuracy differences, and the PMI term, is employed to further encourage predictions within a class to be close to the actual class. The corrected class probabilities and prediction are:

$$\mathbf{p}_m^* = (\omega_{\xi_1^*} p_{m1}, \dots, \omega_{\xi_N^*} p_{mN}) \quad (9)$$

$$\hat{y}_m^* = \arg \max_{n \in \{1, \dots, N\}} \mathbf{p}_m^* \quad (10)$$

3.2 Solving DNIP with Simulated Annealing

Because the NIP objective contains discontinuous functions and is non-differentiable, we solve DNIP by simulated annealing [4, 5]. Simulated annealing (SA) is a Metropolis-Hastings sampling algorithm, which is widely adopted to solve optimization problems with its versatility in dealing with nonlinear models and many constraints [6]. The DNIP mathematical model is nonlinear, so SA is suitable. The main advantage of SA is escaping from local optima and finding global optima after reaching local optima, which is helpful in finding optimal correction weights.

In details, the SA algorithm consists of searching the solution space starting from a randomly initialized ξ and generating a new one by perturbing it. The new solution is either accepted or rejected by the Metropolis criterion after evaluating the DNIP objective. Algorithm 1 describes the searching for optimal ξ using SA. The outer loop performs the cooling/annealing process. In this work, the cooling schedule is set with a geometric decay with $\alpha = 0.95$ and initial temperature of 200,000. The inner loop simulates the thermal equilibrium reaching process at a temperature, and the criterion ensures that either the number of generated or accepted solutions at a temperature is above a threshold [7]. We sample a new ξ from the neighborhood by randomly substitute a selection in ξ . The computational complexity for SA is $\mathcal{O}(NK)$. Please refer to Appendix C for derivations.

4 Experiments

4.1 Experimental Setup

Evaluation Tasks. We evaluate on a diverse set of binary and multi-class NLP classification tasks, across general domains and biomedical domains. The five general-domain evaluation datasets are 4-way news topic classification AGNews, 14-way ontology classification DBpedia [8], 5-way sentiment classification SST-5 [9], 6-way retrieval question classification TREC, binary entailment recognition RTE [10]; the two domain-specific datasets from BLURB [11] are 5-way biomedical relation extraction DDI [12], and 3-way biomedical question answering PubMedQA [13]. The selected biomedical tasks are of practical uses. For example, detecting DDI is useful in preventing adverse effects from drug combinations. Each dataset comes with a training and a test set. We take the full or subset of the training set and obtain ICL class probabilities with ground-truth labels as the optimization set for DNIP optimization. Evaluations are performed on each test set against COBias and overall accuracy. Optimization and dev splits can be found in Appendix D.

Models and Experimental Configuration. We evaluate three open-source LLMs across varied scales and families, including GPT-2-XL (1.5B parameters), Llama-2-7B, and Llama-2-13B. We do few-shot prompting on an NVIDIA A100 GPU, main results use 1-shot prompting, and we also perform more few-shot analyses. For DNIP, β , τ , K , μ are tuned on the development set. To account for variance caused by demonstrations in prompts, we perform three runs for each dataset with different 1-shot demonstrations (randomly selected from the optimization set). Average accuracy and COBias over the three runs are reported. Simulated annealing executes on CPU.

Model	Eval. Metric	AGNews	DBpedia	SST-5	TREC	RTE	DDI	PubMedQA	Avg.
<i>I-shot ICL</i>									
<i>DNIP</i>									
GPT-2-XL	Acc	52.1 _{5.4}	31.8 _{9.9}	34.9 _{13.7}	27.4 _{10.5}	55.4 _{1.9}	14.5 _{4.4}	55.2 _{0.0}	38.8
	COBias	35.5 _{11.5}	40.0 _{3.6}	48.7 _{5.4}	45.6 _{8.7}	82.4 _{24.5}	40.7 _{5.9}	59.4 _{12.6}	50.3
Llama-2-7B	Acc	86.4 _{2.5}	88.9 _{2.0}	42.1 _{11.1}	66.7 _{6.6}	66.3 _{4.3}	6.7 _{0.4}	40.3 _{6.7}	56.8
	COBias	14.0 _{6.5}	13.5 _{2.1}	55.6 _{1.5}	33.2 _{10.0}	61.6 _{10.5}	41.4 _{1.7}	40.9 _{16.1}	37.2
Llama-2-13B	Acc	79.9 _{7.0}	88.6 _{1.7}	44.9 _{4.3}	68.5 _{10.8}	71.5 _{2.2}	7.2 _{0.9}	55.1 _{2.9}	59.4
	COBias	28.3 _{16.1}	16.2 _{3.7}	53.1 _{5.0}	35.9 _{6.5}	43.4 _{7.0}	45.6 _{5.9}	61.2 _{1.9}	40.5

Table 3: Performance comparisons between the 1-shot ICL approach and DNIP. In each cell, we report the average test accuracy/COBias (%) and standard deviation over three different prompts. DNIP greatly improves test accuracy and significantly lowers test COBias upon the ICL approach.

4.2 Main Results

Averaged test accuracy (in black) and COBias (in blue) with standard deviation over three runs are shown in Table 3. Seen from the ICL COBias scores, class accuracy imbalance exists in LLMs of different sizes and families. With DNIP, test COBias is significantly reduced by an absolute 29%, 23%, and 26% for the three models respectively; test accuracy is improved by 16%, 12%, and 10% respectively. For tasks whose ICL test accuracy is already in higher 80s, e.g., DBpedia, DNIP can reduce COBias while further improving the accuracy to 90s. In addition, ICL COBias is very large (82.4%) on GPT-2-XL for RTE, reflecting severe under-predictions in class *False*. After applying corrections, its COBias greatly reduces to 7.1%, demonstrating DNIP’s capability for balancing very imbalanced class accuracies without hurting the overall accuracy much. DNIP is also effective for biomedical tasks, bringing an average absolute reduction of 31% and 13% in COBias, and an average absolute increase of 34% and 11% in accuracy.

Moreover, the 13B Llama model can suffer even higher COBias than its 7B counterpart on biomedical tasks, further showing that class accuracy imbalance does not go away as model sizes increase, and DNIP is effective to balance class accuracies for LLMs of all sizes. Furthermore, we present the confusion matrix of DNIP debiased AGNews results in Table 2. Under-predictions in *Tech* are greatly reduced, with its accuracy significantly improved from 19% to 84%. Additionally, DNIP requires only a small optimization set of 10 examples for a fair improvement in both COBias and accuracy, and it exhibits a further, emergent COBias reduction at several thousands optimization examples. We discuss performance improvements vs. the number of optimization examples needed in Appendix E.

Computational Time. On all datasets, the optimization is finished in the scale of minutes. Though computational time increases with more classes and a more fine-grained weight scale, the time elapsed in optimization for the datasets evaluated in this work is dozens of minutes, even for DBpedia of 14 classes; and a weight scale of 30 is good enough for most of these datasets. This demonstrates the practicality of DNIP as an inference-time debiasing method without incurring much computational costs.

4.3 More ICL Settings

Prompting Method	Metric	AGNews	DBpedia	SST-5	TREC	RTE	DDI	PubMedQA	Avg.
5-shot ICL	Acc	82.5 _{2.0}	93.6 _{1.3}	45.8 _{6.0}	58.7 _{23.3}	61.9 _{16.9}	34.1 _{42.1}	70.4 _{7.1}	63.9
	COBias	24.4 _{4.2}	9.0 _{2.0}	48.0 _{15.4}	35.4 _{13.7}	61.3 _{40.4}	44.4 _{5.4}	52.2 _{19.3}	39.2
DNIP	Acc	88.5 _{0.6}	95.8 _{0.7}	52.9 _{2.5}	76.6 _{8.7}	75.8 _{4.5}	54.1 _{5.1}	59.9 _{1.4}	71.9
	COBias	7.0 _{0.9}	5.7 _{1.1}	15.8 _{12.6}	14.4 _{7.5}	3.1 _{1.9}	16.5 _{7.6}	9.6 _{4.6}	10.3
k-shot (1 demon. per class) ICL	Acc	83.5 _{1.5}	95.2 _{1.2}	50.3 _{2.3}	67.0 _{12.7}	75.0 _{0.8}	9.7 _{1.0}	52.3 _{5.3}	61.9
DNIP	Acc	14.9 _{5.1}	7.0 _{2.2}	36.3 _{7.2}	38.2 _{5.1}	22.5 _{13.2}	39.7 _{3.5}	20.9 _{4.2}	25.6
	COBias	7.3 _{0.5}	4.3 _{0.7}	2.8 _{1.5}	12.1 _{5.5}	5.0 _{3.3}	12.5 _{4.3}	8.7 _{1.2}	7.5

Table 4: DNIP results in more ICL settings. Average score over three runs are reported.

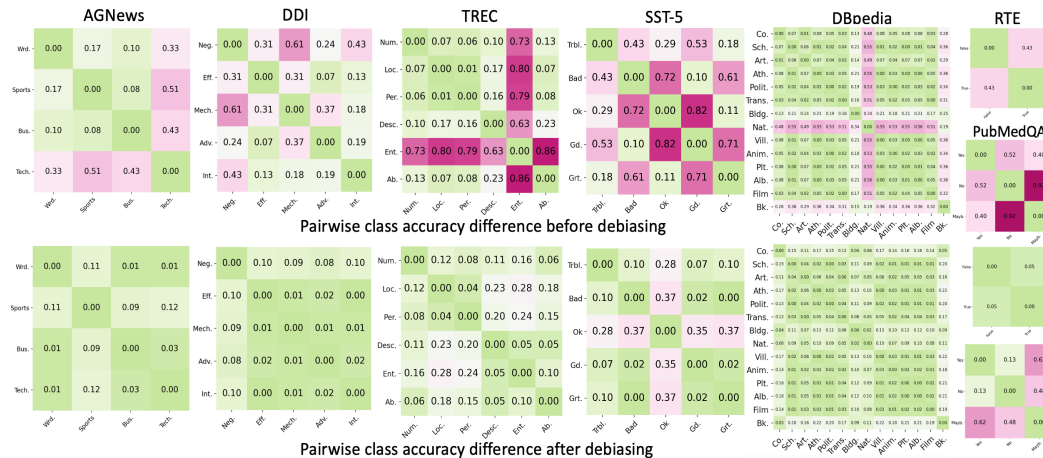


Figure 3: Pairwise class accuracy differences on test sets before and after DNIP; the **pinker** the higher difference, the **greener** the lower; averaged over three runs. DNIP achieves nearly 0 accuracy differences for many class pairs.

We prompt Llama-2-13B in two additional settings: 5-shot, where each demonstration is randomly selected; k-shot, where k is the number of classes and each class is represented by a demonstration, randomly selected. Table 4 shows that, for example, the relative average COBias reduction by DNIP is 65% and 74% for 1-shot (Table 3) and 5-shot respectively, with relative average accuracy increase of 16% and 11%. The rationale is, demonstrations contribute to variance in outputs, but prompt engineering alone does not mitigate much the imbalance. DNIP can correct the outputs no matter what different starting points are given.

4.4 DNIP Significantly Balances Class Accuracies for Classification Tasks with as Many as 14 Classes

We further investigate DBpedia (14 classes). Before debiasing, class *Nat.* exhibits the largest accuracy difference compared to others. In fact, *Nat.* is the most under-predicted class, whose odd class is *Trans.* and second odd class is *Bldg.*, as shown by the confusion matrix in Figure 2 (using the seed 0 run). DNIP greatly reduces wrong *Trans.* and *Bldg.* predictions for *Nat.*. Moreover, when averaged over all three runs, test accuracy for *Nat.* improves from 44% to 89%, and that for *Trans.*

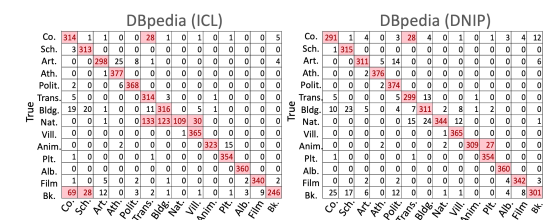
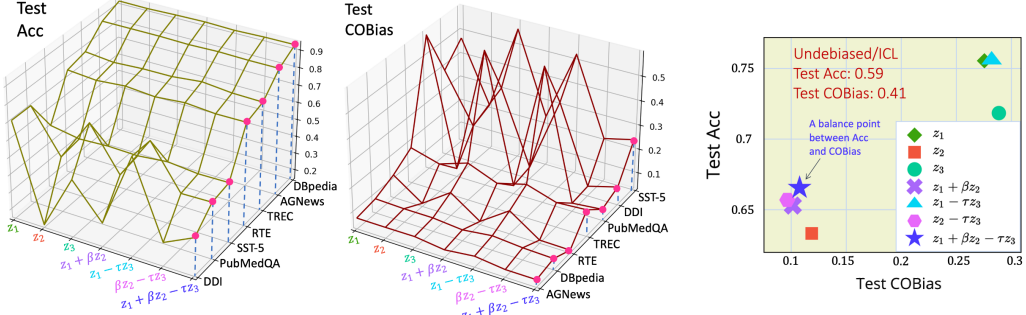


Figure 2: Test confusion matrix for DBpedia before and after applying DNIP. DNIP greatly improves ICL predictions for *Nat.*, which is the most under-predicted class by ICL.

also increases from 78% to 87%, demonstrating that DNIP’s competence in reducing class accuracy differences for tasks with as many as 14 classes.

We also visualize pairwise class accuracy differences before and after applying DNIP to 1-shot, Llama-2-13B ICL results in Figure 3. In each heatmap, row i , column j cell represents the absolute difference between the test accuracies of two classes in row i, j , i.e., $|A_{c_i} - A_{c_j}|$. DNIP brings the accuracy differences down to close to zero for AGNews, DDI, DBpedia, and RTE. The lighter green heatmaps in the bottom row show that DNIP consistently reduces COBias across different NLP classification tasks. Furthermore, we present more heatmaps for smaller LLMs including Llama-2-7B and GPT-2-XL in Appendix F.



With $z_1 + \beta z_2 - \tau z_3$, COBias reduces by 30% and Acc increases by 8%, and all datasets achieve a balance between Acc and COBias, where AGNews, DBpedia each obtains its lowest COBias and highest Acc, RTE obtains its lowest COBias and second highest Acc, and the rest of the four datasets obtain a low COBias with a fair Acc. Notably, the accuracy-related objectives alone can raise Acc from 59% to over 75%, but COBias reduction is 13%.

Figure 4: Ablation analysis of the objective function, exemplified with Llama-2-13B; test scores averaged over 7 datasets are used for the rightmost plot.

4.5 Accuracy-related Objectives vs. COBias Objective

We show that the integration of accuracy-related objectives and the COBias objective are indispensable in achieving the best of both worlds in Figure 4. DNIP objective function z consists of three terms: the error rate term $z_1 = \frac{1}{M} \sum_{m=1}^M \mathbb{1}\{\hat{y}_m \neq y_m\}$; the COBias term $z_2 = \binom{N}{2}^{-1} \sum_{i=1}^{N-1} \sum_{j=i+1}^N |A_{c_i} - A_{c_j}|$; and the PMI term $z_3 = \sum_{j=1}^N \text{PMI}_j$; the accuracy-related terms are z_1 and z_3 . We ablate all ablation objective functions to perform DNIP: $z_1, z_2, z_3, z_1 + \beta z_2, z_1 - \tau z_3, \beta z_2 - \tau z_3, z_1 + \beta z_2 - \tau z_3$. Ablations on GPT-2-XL and Llama-2-7B show similar findings (Appendix G). To make fair comparisons, we fix $\beta = 2.7, \tau = 0.2$ and weight scale $K = 30$, which may not result in the same scores reported in Table 3. Among all ablations, $z_1 + \beta z_2 - \tau z_3$ achieves a balance point between accuracy and COBias. For the criteria, lower COBias is our top priority; when COBias scores are similarly low, we prefer the one that achieves higher accuracy. Compared to $z_1 + \beta z_2 - \tau z_3$: (1) Using z_1 or z_3 solely emphasizes improving accuracy; though obtaining higher or similar accuracy, they suffer a higher COBias. (2) Using $z_1 - \tau z_3$ also obtains a higher/similar accuracy but a higher COBias. (3) Using z_2 solely focuses on mitigating COBias and is straightforwardly effective in reducing COBias, but the shortcoming is a lower accuracy. (4) Using $z_1 + \beta z_2$ or $\beta z_2 - \tau z_3$ is promising with a similar/lower accuracy and a lower COBias. Accuracy-related objectives alone increase accuracy by over 16% (75% – 59%), suggesting DNIP is effective for those who emphasize accuracy improvement.

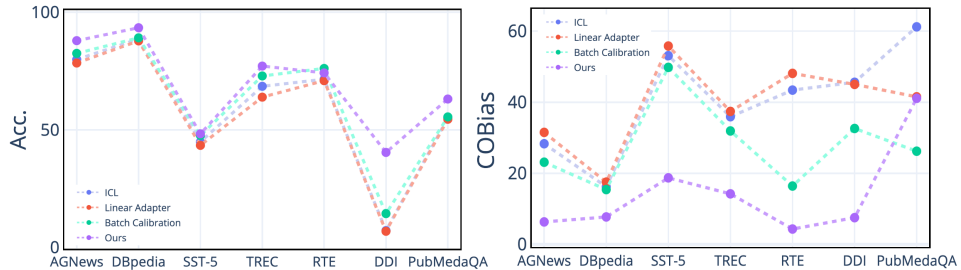


Figure 5: Comparisons to more methods.

4.6 Optimizing COBias_{single}

Using COBias_{single} (Eq. 3) for DNIP optimization will focus on odd classes only. Figure 6 shows ablation results when replacing the COBias term in the DNIP objective with COBias_{single}. Blue dots represent the respective evaluation metric score of the original 1-shot ICL Llama-2-13B outputs of the seven benchmark datasets; green dots are debiased results optimized by the COBias_{single} DNIP objective; red dots are results optimized by the COBias DNIP objective.

Comparing DNIP with COBias_{single} and DNIP with COBias, their performances are close, but DNIP with COBias achieves higher overall test accuracy and slightly better bias mitigation performances. In other words, DNIP with COBias_{single} can significantly minimize accuracy differences between odd classes and ground-truth classes, but DNIP with COBias is even more effective when it comes to balancing all pairs of classes, not limited to the odd classes.

5 Related Work

Class accuracy imbalance is one of the potential failures of LLMs. Analysis towards understanding LLM failure modes has gained remarkable insights. For example, understanding hallucinations in LLMs facilitates fact-checking metrics for LLMs.[14, 15, 16]. Jones and Steinhardt [17] reveals failure modes of LLMs which resemble cognitive biases. Lu et al. [18] identify order sensitivity in prompting. The class accuracy imbalance has multi-faceted causes, from pre-training data, such as predilections for common tokens in pretraining [19], to a liking for specific patterns or answers [20]. Other causes include choices of prompt templates [21, 22, 23], demonstrations [24], and prompt orders [25]. Unintended LLM behaviors may also exacerbate it, such as sycophancy[26, 27, 28].

6 Discussion

More Methods That Potentially Improve Accuracy while Reducing COBias. Prior methods tackle the prediction bias problem from different angles. Although COBias is not explicitly modeled, they are promising to reduce COBias. Therefore, we draw comparisons to two popular categories of debiasing methods, adaptations and calibrations. In particular, with the same class probability vectors as input, we build a single linear adapter (LA) network with adapter dimension of 64, and train it towards the same objective as DNIP; we also follow the batch calibration method [29] to estimate a calibration term using test examples. Figure 5 shows the comparison results. fine-tuning a simple linear adapter does not work well on the class output probabilities. The proposed method outperforms both methods in accuracy and COBias.

Evaluating Closed LLMs. While closed LLMs such as ChatGPT [30] are interesting to debias, ChatGPT returns log probabilities of top 20 most likely tokens, which may not cover the probability for every class that is needed as inputs to DNIP.

Appendix H has more discussions on optimization algorithms for integer programming, how our motivation is different from other classical post-hoc correction methods, using calibration methods to mitigate ICL biases, and using Chain-of-Thought prompting to improve LLM predictions.

7 Conclusion

We introduce COBias to quantify class accuracy imbalance for language models, and emphasize the need to minimize COBias to push for more reliable predictions while maintaining good overall accuracy. We correct ICL output class probabilities towards this goal as a combinatorial optimization problem, proposing DNIP to optimize class correction weights. Evaluations on three LLMs across seven classification tasks demonstrate that DNIP achieves both lower COBias and higher overall accuracy over original ICL results.

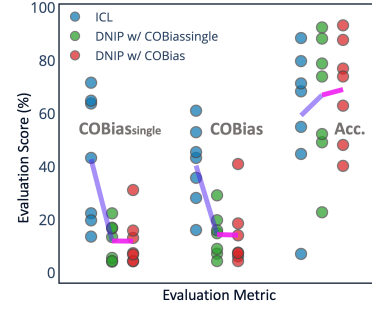


Figure 6: Test COBias_{single}, COBias, and overall accuracy scores (from left to right).

References

- [1] Tom Brown, Benjamin Mann, Nick Ryder, Melanie Subbiah, Jared D Kaplan, Prafulla Dhariwal, Arvind Neelakantan, Pranav Shyam, Girish Sastry, Amanda Askell, Sandhini Agarwal, Ariel Herbert-Voss, Gretchen Krueger, Tom Henighan, Rewon Child, Aditya Ramesh, Daniel Ziegler, Jeffrey Wu, Clemens Winter, Chris Hesse, Mark Chen, Eric Sigler, Mateusz Litwin, Scott Gray, Benjamin Chess, Jack Clark, Christopher Berner, Sam McCandlish, Alec Radford, Ilya Sutskever, and Dario Amodei. Language Models are Few-Shot Learners. In *Advances in Neural Information Processing Systems*, pages 1877–1901, 2020. URL https://proceedings.neurips.cc/paper_files/paper/2020/file/1457c0d6bfc4967418bfb8ac142f64a-Paper.pdf.
- [2] Xiang Zhang, Junbo Zhao, and Yann LeCun. Character-level Convolutional Networks for Text Classification. In *Advances in Neural Information Processing Systems*, 2015. URL https://proceedings.neurips.cc/paper_files/paper/2015/file/250cf8b51c773f3f8dc8b4be867a9a02-Paper.pdf.
- [3] Xin Li and Dan Roth. Learning Question Classifiers. In *COLING 2002: The 19th International Conference on Computational Linguistics*, 2002. URL <https://aclanthology.org/C02-1150>.
- [4] S. Kirkpatrick, C. D. Gelatt, and M. P. Vecchi. Optimization by Simulated Annealing. *Science*, pages 671–680, 1983. URL <https://www.science.org/doi/abs/10.1126/science.220.4598.671>.
- [5] Richard W. Eglese. Simulated Annealing: A Tool for Operational Research. *European Journal of Operational Research*, pages 271–281, 1990. URL <https://www.sciencedirect.com/science/article/pii/037722179090001R>.
- [6] Franco Busetti. *Simulated Annealing Overview*. 05 2001. URL https://www.researchgate.net/publication/238690391_Simulated_annealing_overview.
- [7] Fabio Romeo and Alberto Sangiovanni-Vincentelli. A Theoretical Framework for Simulated Annealing. *Algorithmica*, pages 302–345, 1991. URL <https://link.springer.com/article/10.1007/BF01759049>.
- [8] Sören Auer, Christian Bizer, Georgi Kobilarov, Jens Lehmann, Richard Cyganiak, and Zachary Ives. DBpedia: A Nucleus for A Web of Open Data. In *Proceedings of the 6th International The Semantic Web and 2nd Asian Conference on Asian Semantic Web Conference*, page 722–735, 2007.
- [9] Richard Socher, Alex Perelygin, Jean Wu, Jason Chuang, Christopher D. Manning, Andrew Ng, and Christopher Potts. Recursive Deep Models for Semantic Compositionality Over a Sentiment Treebank. In *Proceedings of the 2013 Conference on Empirical Methods in Natural Language Processing*, pages 1631–1642, 2013. URL <https://aclanthology.org/D13-1170>.
- [10] Ido Dagan, Oren Glickman, and Bernardo Magnini. The PASCAL Recognising Textual Entailment Challenge. In *Machine Learning Challenges. Evaluating Predictive Uncertainty, Visual Object Classification, and Recognising Tectual Entailment*, pages 177–190, 2006.
- [11] Yu Gu, Robert Tinn, Hao Cheng, Michael Lucas, Naoto Usuyama, Xiaodong Liu, Tristan Naumann, Jianfeng Gao, and Hoifung Poon. Domain-Specific Language Model Pretraining for Biomedical Natural Language Processing. *ACM Trans. Comput. Healthcare*, 2021. URL <https://doi.org/10.1145/3458754>.
- [12] Isabel Segura-Bedmar, Paloma Martínez, and María Herrero-Zazo. SemEval-2013 Task 9 : Extraction of Drug-Drug Interactions from Biomedical Texts (DDIExtraction 2013). In *Second Joint Conference on Lexical and Computational Semantics (*SEM), Volume 2: Proceedings of the Seventh International Workshop on Semantic Evaluation (SemEval 2013)*, pages 341–350, 2013. URL <https://aclanthology.org/S13-2056.pdf>.

[13] Qiao Jin, Bhuwan Dhingra, Zhengping Liu, William Cohen, and Xinghua Lu. PubMedQA: A Dataset for Biomedical Research Question Answering. In *Proceedings of the 2019 Conference on Empirical Methods in Natural Language Processing and the 9th International Joint Conference on Natural Language Processing (EMNLP-IJCNLP)*, pages 2567–2577, 2019. URL <https://aclanthology.org/D19-1259>.

[14] Ziwei Ji, Nayeon Lee, Rita Frieske, Tiezheng Yu, Dan Su, Yan Xu, Etsuko Ishii, Ye Jin Bang, Andrea Madotto, and Pascale Fung. Survey of Hallucination in Natural Language Generation. *ACM Comput. Surv.*, 2023. URL <https://doi.org/10.1145/3571730>.

[15] Bhuwan Dhingra, Manaal Faruqui, Ankur Parikh, Ming-Wei Chang, Dipanjan Das, and William Cohen. Handling Divergent Reference Texts when Evaluating Table-to-Text Generation. In *Proceedings of the 57th Annual Meeting of the Association for Computational Linguistics*, pages 4884–4895, 2019. URL <https://aclanthology.org/P19-1483>.

[16] Zhijiang Guo, Michael Schlichtkrull, and Andreas Vlachos. A Survey on Automated Fact-Checking. *Transactions of the Association for Computational Linguistics*, pages 178–206, 2022. URL <https://aclanthology.org/2022.tacl-1.11>.

[17] Erik Jones and Jacob Steinhardt. Capturing Failures of Large Language Models via Human Cognitive Biases. In *Advances in Neural Information Processing Systems*, pages 11785–11799, 2022. URL https://proceedings.neurips.cc/paper_files/paper/2022/file/4d13b2d99519c5415661dad44ab7edcd-Paper-Conference.pdf.

[18] Yao Lu, Max Bartolo, Alastair Moore, Sebastian Riedel, and Pontus Stenetorp. Fantastically Ordered Prompts and Where to Find Them: Overcoming Few-Shot Prompt Order Sensitivity. In *Proceedings of the 60th Annual Meeting of the Association for Computational Linguistics (Volume 1: Long Papers)*, pages 8086–8098, 2022. URL <https://aclanthology.org/2022.acl-long.556>.

[19] Zihao Zhao, Eric Wallace, Shi Feng, Dan Klein, and Sameer Singh. Calibrate Before Use: Improving Few-shot Performance of Language Models. In *Proceedings of the 38th International Conference on Machine Learning*, pages 12697–12706, 2021. URL <https://proceedings.mlr.press/v139/zhao21c.html>.

[20] Nora Kassner and Hinrich Schütze. Negated and Misprimed Probes for Pretrained Language Models: Birds Can Talk, But Cannot Fly. In *Proceedings of the 58th Annual Meeting of the Association for Computational Linguistics*, pages 7811–7818, 2020. URL <https://aclanthology.org/2020.acl-main.698>.

[21] Zhengbao Jiang, Frank F. Xu, Jun Araki, and Graham Neubig. How Can We Know What Language Models Know? *Transactions of the Association for Computational Linguistics*, pages 423–438, 2020. URL <https://aclanthology.org/2020.tacl-1.28>.

[22] Sewon Min, Xinxi Lyu, Ari Holtzman, Mikel Artetxe, Mike Lewis, Hannaneh Hajishirzi, and Luke Zettlemoyer. Rethinking the Role of Demonstrations: What Makes In-Context Learning Work? In *Proceedings of the 2022 Conference on Empirical Methods in Natural Language Processing*, pages 11048–11064, 2022. URL <https://aclanthology.org/2022.emnlp-main.759>.

[23] Xinxi Lyu, Sewon Min, Iz Beltagy, Luke Zettlemoyer, and Hannaneh Hajishirzi. Z-ICL: Zero-Shot In-Context Learning with Pseudo-Demonstrations. In *Proceedings of the 61st Annual Meeting of the Association for Computational Linguistics (Volume 1: Long Papers)*, pages 2304–2317, July 2023. URL <https://aclanthology.org/2023.acl-long.129>.

[24] Ari Holtzman, Peter West, Vered Shwartz, Yejin Choi, and Luke Zettlemoyer. Surface Form Competition: Why the Highest Probability Answer Isn’t Always Right. In *Proceedings of the 2021 Conference on Empirical Methods in Natural Language Processing*, pages 7038–7051, 2021. URL <https://aclanthology.org/2021.emnlp-main.564>.

[25] Miles Turpin, Julian Michael, Ethan Perez, and Samuel Bowman. Language Models Don’t Always Say What They Think: Unfaithful Explanations in Chain-of-Thought

Prompting. In *Advances in Neural Information Processing Systems*, pages 74952–74965, 2023. URL https://proceedings.neurips.cc/paper_files/paper/2023/file/ed3fea9033a80fea1376299fa7863f4a-Paper-Conference.pdf.

- [26] Ethan Perez, Sam Ringer, Kamile Lukosiute, Karina Nguyen, Edwin Chen, Scott Heiner, Craig Pettit, Catherine Olsson, Sandipan Kundu, Saurav Kadavath, Andy Jones, Anna Chen, Benjamin Mann, Brian Israel, Bryan Seethor, Cameron McKinnon, Christopher Olah, Da Yan, Daniela Amodei, Dario Amodei, Dawn Drain, Dustin Li, Eli Tran-Johnson, Guro Khundadze, Jackson Kernion, James Landis, Jamie Kerr, Jared Mueller, Jeeyoon Hyun, Joshua Landau, Kamal Ndousse, Landon Goldberg, Liane Lovitt, Martin Lucas, Michael Sellitto, Miranda Zhang, Neerav Kingsland, Nelson Elhage, Nicholas Joseph, Noemi Mercado, Nova DasSarma, Oliver Rausch, Robin Larson, Sam McCandlish, Scott Johnston, Shauna Kravec, Sheer El Showk, Tamera Lanham, Timothy Telleen-Lawton, Tom Brown, Tom Henighan, Tristan Hume, Yuntao Bai, Zac Hatfield-Dodds, Jack Clark, Samuel R. Bowman, Amanda Askell, Roger Grosse, Danny Hernandez, Deep Ganguli, Evan Hubinger, Nicholas Schiefer, and Jared Kaplan. Discovering Language Model Behaviors with Model-Written Evaluations. In *Findings of the Association for Computational Linguistics: ACL 2023*, pages 13387–13434, 2023. URL <https://aclanthology.org/2023.findings-acl.847>.
- [27] Mrinank Sharma, Meg Tong, Tomasz Korbak, David Duvenaud, Amanda Askell, Samuel R. Bowman, Esin DURMUS, Zac Hatfield-Dodds, Scott R Johnston, Shauna M Kravec, Timothy Maxwell, Sam McCandlish, Kamal Ndousse, Oliver Rausch, Nicholas Schiefer, Da Yan, Miranda Zhang, and Ethan Perez. Towards Understanding Sycophancy in Language Models. In *The Twelfth International Conference on Learning Representations*, 2024. URL <https://openreview.net/forum?id=tvhaxkMKAn>.
- [28] Jerry Wei, Da Huang, Yifeng Lu, Denny Zhou, and Quoc V. Le. Simple synthetic data reduces sycophancy in large language models, 2024. URL <https://arxiv.org/abs/2308.03958>.
- [29] Han Zhou, Xingchen Wan, Lev Proleev, Diana Mincu, Jilin Chen, Katherine A Heller, and Subhrajit Roy. Batch Calibration: Rethinking Calibration for In-Context Learning and Prompt Engineering. In *The Twelfth International Conference on Learning Representations*, 2024. URL <https://openreview.net/forum?id=L3FHM0KZcS>.
- [30] OpenAI, Josh Achiam, Steven Adler, Sandhini Agarwal, Lama Ahmad, Ilge Akkaya, Florencia Leoni Aleman, Diogo Almeida, Janko Altenschmidt, Sam Altman, Shyamal Anadkat, Red Avila, Igor Babuschkin, Suchir Balaji, Valerie Balcom, Paul Baltescu, Haiming Bao, Mohammad Bavarian, Jeff Belgum, Irwan Bello, Jake Berdine, Gabriel Bernadett-Shapiro, Christopher Berner, Lenny Bogdonoff, Oleg Boiko, Madelaine Boyd, Anna-Luisa Brakman, Greg Brockman, Tim Brooks, Miles Brundage, Kevin Button, Trevor Cai, Rosie Campbell, Andrew Cann, Brittany Carey, Chelsea Carlson, Rory Carmichael, Brooke Chan, Che Chang, Fotis Chantzis, Derek Chen, Sully Chen, Ruby Chen, Jason Chen, Mark Chen, Ben Chess, Chester Cho, Casey Chu, Hyung Won Chung, Dave Cummings, Jeremiah Currier, Yunxing Dai, Cory Decareaux, Thomas Degry, Noah Deutsch, Damien Deville, Arka Dhar, David Dohan, Steve Dowling, Sheila Dunning, Adrien Ecoffet, Atty Eleti, Tyna Eloundou, David Farhi, Liam Fedus, Niko Felix, Simón Posada Fishman, Juston Forte, Isabella Fulford, Leo Gao, Elie Georges, Christian Gibson, Vik Goel, Tarun Gogineni, Gabriel Goh, Rapha Gontijo-Lopes, Jonathan Gordon, Morgan Grafstein, Scott Gray, Ryan Greene, Joshua Gross, Shixiang Shane Gu, Yufei Guo, Chris Hallacy, Jesse Han, Jeff Harris, Yuchen He, Mike Heaton, Johannes Heidecke, Chris Hesse, Alan Hickey, Wade Hickey, Peter Hoeschele, Brandon Houghton, Kenny Hsu, Shengli Hu, Xin Hu, Joost Huizinga, Shantanu Jain, Shawn Jain, Joanne Jang, Angela Jiang, Roger Jiang, Haozhun Jin, Denny Jin, Shino Jomoto, Billie Jonn, Heewoo Jun, Tomer Kaftan, Łukasz Kaiser, Ali Kamali, Ingmar Kanitscheider, Nitish Shirish Keskar, Tabarak Khan, Logan Kilpatrick, Jong Wook Kim, Christina Kim, Yongjik Kim, Jan Hendrik Kirchner, Jamie Kiros, Matt Knight, Daniel Kokotajlo, Łukasz Kondraciuk, Andrew Kondrich, Aris Konstantinidis, Kyle Kosic, Gretchen Krueger, Vishal Kuo, Michael Lampe, Ikai Lan, Teddy Lee, Jan Leike, Jade Leung, Daniel Levy, Chak Ming Li, Rachel Lim, Molly Lin, Stephanie Lin, Mateusz Litwin, Theresa Lopez, Ryan Lowe, Patricia Lue, Anna Makanju, Kim Malfacini, Sam Manning, Todor Markov, Yaniv Markovski, Bianca Martin, Katie Mayer, Andrew Mayne, Bob McGrew, Scott Mayer McKinney, Christine McLeavey, Paul McMillan, Jake McNeil, David Medina, Aalok Mehta, Jacob Menick, Luke Metz, Andrey Mishchenko, Pamela Mishkin, Vinnie

Monaco, Evan Morikawa, Daniel Mossing, Tong Mu, Mira Murati, Oleg Murk, David Mély, Ashvin Nair, Reiichiro Nakano, Rajeev Nayak, Arvind Neelakantan, Richard Ngo, Hyeonwoo Noh, Long Ouyang, Cullen O’Keefe, Jakub Pachocki, Alex Paino, Joe Palermo, Ashley Pantuliano, Giambattista Parascandolo, Joel Parish, Emry Parparita, Alex Passos, Mikhail Pavlov, Andrew Peng, Adam Perelman, Filipe de Avila Belbute Peres, Michael Petrov, Henrique Ponde de Oliveira Pinto, Michael Pokorny, Michelle Pokrass, Vitchyr H. Pong, Tolly Powell, Alethea Power, Boris Power, Elizabeth Proehl, Raul Puri, Alec Radford, Jack Rae, Aditya Ramesh, Cameron Raymond, Francis Real, Kendra Rimbach, Carl Ross, Bob Rotstod, Henri Roussez, Nick Ryder, Mario Saltarelli, Ted Sanders, Shibani Santurkar, Girish Sastry, Heather Schmidt, David Schnurr, John Schulman, Daniel Selsam, Kyla Sheppard, Toki Sherbakov, Jessica Shieh, Sarah Shoker, Pranav Shyam, Szymon Sidor, Eric Sigler, Maddie Simens, Jordan Sitkin, Katarina Slama, Ian Sohl, Benjamin Sokolowsky, Yang Song, Natalie Staudacher, Felipe Petroski Such, Natalie Summers, Ilya Sutskever, Jie Tang, Nikolas Tezak, Madeleine B. Thompson, Phil Tillet, Amin Tootoonchian, Elizabeth Tseng, Preston Tuggle, Nick Turley, Jerry Tworek, Juan Felipe Cerón Uribe, Andrea Vallone, Arun Vijayvergiya, Chelsea Voss, Carroll Wainwright, Justin Jay Wang, Alvin Wang, Ben Wang, Jonathan Ward, Jason Wei, CJ Weinmann, Akila Welihinda, Peter Welinder, Jiayi Weng, Lilian Weng, Matt Wiethoff, Dave Willner, Clemens Winter, Samuel Wolrich, Hannah Wong, Lauren Workman, Sherwin Wu, Jeff Wu, Michael Wu, Kai Xiao, Tao Xu, Sarah Yoo, Kevin Yu, Qiming Yuan, Wojciech Zaremba, Rowan Zellers, Chong Zhang, Marvin Zhang, Shengjia Zhao, Tianhao Zheng, Juntang Zhuang, William Zhuk, and Barret Zoph. Gpt-4 technical report, 2024. URL <https://arxiv.org/abs/2303.08774>.

- [31] OpenAI. Chatgpt: A large-scale pretrained dialogue model for generating conversational text. *OpenAI Blog*, 2022. URL <https://openai.com/blog/chatgpt>.
- [32] Mirac Suzgun, Nathan Scales, Nathanael Schärli, Sebastian Gehrmann, Yi Tay, Hyung Won Chung, Aakanksha Chowdhery, Quoc Le, Ed Chi, Denny Zhou, and Jason Wei. Challenging BIG-Bench Tasks and Whether Chain-of-Thought Can Solve Them. In *Findings of the Association for Computational Linguistics: ACL 2023*, pages 13003–13051, 2023. URL <https://aclanthology.org/2023.findings-acl.824>.

	<i>Pred.</i>				
	Neg	Eff	Mech	Adv	Int
Neg	1749	438	1498	546	506
Eff	118	33	110	52	47
True Mech	77	28	123	45	29
Adv	84	15	62	36	24
Int	34	11	28	13	10

Table 5: Over-prediction and under-prediction in Llama-2-13B, as shown by the confusion matrix on DDI test set.

	<i>Pred.</i>				
	Neg	Eff	Mech	Adv	Int
Neg	809	707	1001	217	2003
Eff	45	109	79	6	121
True Mech	15	46	172	0	69
Adv	24	12	18	79	88
Int	9	9	7	1	70

Table 6: Over-prediction and under-prediction in ChatGPT, as shown by the confusion matrix on DDI test set.

A Other Examples of Over-prediction and Under-prediction in LLMs

We present Llama-2-13B’s and ChatGPT’s over- and under-predictions on a class imbalanced classification task, the Drug-Drug Interaction (DDI) relation classification task, where around 90% test instances are *Negative*. As shown in Table 5, Llama-2-13B significantly under-predicts *Negative*. In Table 6, similar under-predictions in the DDI *Negative* class happens for ChatGPT (GPT-3.5-turbo-instruct [31]), the RLHF’d chat LLM with magnitudes of more parameters. (It is noted that at the time of our experiments, ChatGPT does not support returning full probabilities over the entire vocabulary. To investigate the over-/under-prediction issue, we prompt ChatGPT on the DDI task with the following prompt template: “Please choose one most suitable answer for the following description. [ONE-SHOT DEMONSTRATION] Description: [TEST INPUT] Q: What is the drug-drug interaction relation between the aforementioned @DRUG\$ pair? Choose from *Negative*, *Mechanism*, *Effect*, *Advice*, *Interaction*. A: ”, and use the answer token directly as the prediction, and plot the confusion matrix in Table 6. For fair comparisons, we prompt Llama-2-13B in the same manner to obtain Table 5, which is different from how we prompt Llama-2-13B in the main paper.)

The over-/under-predictions in LLMs of different sizes and families, and the inconveniences in training/fine-tuning LLMs, together call for a more actionable bias metric quantifying the over-/under-prediction issue and an accompanying debiasing method tailored for LLMs.

B Directly Optimizing the Odd Prediction Rate

We discuss another option of measuring class accuracy imbalances, which does not mitigate odd predictions as effective as using COBias, though using it can obtain similar or slightly higher overall accuracy. It is the odd prediction rate, i.e., the rate of odd predictions over the number of ground-truth instances, which is a measurement reflecting the odd class and the level of “accuracy hurt” caused by the odd class. We define $H(c_i)$ as below.

$$H(c_i) = \frac{\sum_m \mathbb{1}\{y_m = c_i, \hat{y}_m = \text{odd}_i\}}{\sum_k \mathbb{1}\{y_k = c_i\}}, \quad (11)$$

where odd_i is the odd class to c_i . For example, one may quantify the effect of a current odd class *Business* to the ground-truth class *Tech* as the rate of *Business* predictions over ground-truth *Tech*

instances, i.e., 822/1240, and an immediate debiasing goal is to minimize this rate. The DNIP objective with the odd prediction rate is as follows.

$$\min Z(\xi) = \frac{1}{M} \sum_{m=1}^M \mathbb{1}\{\hat{y}_m \neq y_m\} + \beta \frac{1}{N} \sum_i H(c_i) - \tau \sum_{j=1}^N \text{PMI}_j \quad (12)$$

We compare the effectiveness of using COBias, COBias_{single}, and H in the DNIP objective, and refer to the respective objectives as Z_{CB} (Eq. 3), Z_{CB_s} , and Z_H (Eq. 12). Detailed test scores for the benchmark datasets on Llama-2-13B, including class accuracies, are shown in Tables 7 to 13.

In short, Z_H still leaves some classes under-predicted, as exemplified by the individual test class accuracies, and test COBias (or test COBias_{single}) scores on TREC, RTE, etc. The rationale is that optimizing bias measurements that extend accuracy differences, such as the odd prediction rates, does not mitigate odd class predictions better than optimizing COBias directly. Z_{CB} most effectively mitigates the over- and under-prediction issue, balancing class accuracies.

Optimizing other extended measurements, such as precision or F_1 scores differences, may obtain similar performances to the three existing metrics, which will be left for future discussions.

DNIP Objective (Results without DNIP are shown on the last row.)	Evaluation Metric														
	CB	CB _s	H	Overall Acc.	Class Acc.										
					Co.	Sch.	Art.	Ath.	Polit.	Trans.	Bldg.	Nat.	Vill.	Anim.	Plt.
Z_{CB}	7.7	7.5	3.3	93.4	82.6	97.7	94.0	99.5	97.9	94.4	86.6	89.0	99.5	96.3	98.5
Z_{CB_s}	9.1	5.7	3.9	92.6	87.4	96.8	97.1	98.9	98.1	87.3	87.6	84.0	99.3	99.2	97.9
Z_H	8.9	9.5	2.8	93.2	76.2	99.3	95.0	99.4	98.8	96.9	82.8	89.8	99.5	98.4	98.9
ICL	16.2	13.7	5.6	88.6	91.7	99.1	92.7	99.7	97.0	94.8	78.4	44.2	99.7	96.9	99.3

Table 7: Comparison of DBpedia test set evaluation scores (%) for three DNIP objective functions Z_{CB} , Z_{CB_s} , and Z_H . Average scores over three runs of different 1-shot demonstrations are reported.

DNIP Objective (Results without DNIP are shown on the last row.)	Evaluation Metric									
	CB	CB _s	H	Overall Acc.	Class Acc.					
					Wrd.	Sports	Bus.	Tech.		
Z_{CB}	6.3	4.4	7.2	87.9	85.3	95.9	86.5	83.9		
Z_{CB_s}	7.3	4.3	6.9	88.4	84.8	98.2	85.8	84.7		
Z_H	8.5	4.8	6.5	88.3	86.8	98.7	84.2	83.2		
ICL	28.3	22.5	14.6	79.9	81.5	98.7	91.0	48.0		

Table 8: Comparison of AGNews test set evaluation scores (%) for three DNIP objective functions Z_{CB} , Z_{CB_s} , and Z_H . Average scores over three runs of different 1-shot demonstrations are reported.

DNIP Objective (Results without DNIP are shown in the last row.)	Evaluation Metric									
	CB	CB _s	H	Overall Acc.	Class Acc.					
					Neg.	Eff.	Mech.	Adv.	Int.	
Z_{CB}	7.5	7.0	39.6	40.4	42.1	31.6	32.8	33.9	31.6	
Z_{CB_s}	19.9	16.8	42.1	22.9	19.9	34.2	37.3	39.8	44.8	
Z_H	43.6	44.6	30.9	21.7	17.6	12.6	47.2	85.5	33.3	
ICL	45.6	71.8	59.4	7.2	0.0	30.7	61.5	24.1	43.5	

Table 9: Comparison of DDI test set evaluation scores (%) for three DNIP objective functions Z_{CB} , Z_{CB_s} , and Z_H . Average scores over three runs of different 1-shot demonstrations are reported.

C Derivation of SA Algorithm Complexity

Given N classes and K scales, the DNIP objective has NK variables. For each inner loop of SA, the length of the Markov chain is often several times of the size of variables, i.e., λNK . For a geometric cooling schedule $T = \alpha^n T_{\max}$, the number of outer-loop iterations is:

DNIP Objective (Results without DNIP are shown in the last row.)	Evaluation Metric							
	CB	CB _s	H	Overall Acc.	Class Acc.			
					Num.	Loc.	Per.	Desc.
Z _{CB}	14.2	16.0	18.9	77.1	80.2	92.2	88.7	69.1
Z _{CB_s}	15.0	13.6	17.7	79.0	90.0	89.3	87.7	70.0
Z _H	21.3	31.7	12.6	77.3	93.8	88.5	91.3	75.6
ICL	35.9	19.9	18.5	68.5	82.9	89.7	88.7	72.9
					9.9		9.9	96.3

Table 10: Comparison of TREC test set evaluation scores (%) for three DNIP objective functions Z_{CB} , Z_{CB_s} , and Z_H . Average scores over three runs of different 1-shot demonstrations are reported.

DNIP Objective (Results without DNIP are shown in the last row.)	Evaluation Metric							
	CB	CB _s	H	Overall Acc.	Class Acc.			
					False	True	False	True
Z _{CB}	4.5	4.5	26.0	74.1	71.8	76.3		
Z _{CB_s}	4.5	4.5	26.0	74.1	71.8	76.3		
Z _H	13.3	13.3	24.7	75.7	68.7	82.0		
ICL	43.4	43.4	29.7	71.5	48.6	92.0		

Table 11: Comparison of RTE test set evaluation scores (%) for three DNIP objective functions Z_{CB} , Z_{CB_s} , and Z_H . Average scores over three runs of different 1-shot demonstrations are reported.

$$N^{\text{outer}} = \log_{\alpha} \frac{T_{\min}}{T_{\max}} \quad (13)$$

The sampling times for the SA algorithm is $\lambda N K \log_{\alpha} (T_{\min}/T_{\max})$. Therefore, the computational complexity is $\mathcal{O}(\lambda N K \log_{\alpha} (T_{\min}/T_{\max})) = \mathcal{O}(NK)$.

In addition, the brute force strategy to find optimal correction weights is enumerated search, where the number of weight combinations to explore is K^N for an example; for M examples, it results in a computational complexity of $\mathcal{O}(K^N \cdot M)$, which can not finish in polynomial time. When M or N is large, enumerated search is computationally intensive. Considering this, we did not adopt the brute force strategy.

D Dataset Preprocessing

We take the full training set and obtain ICL class probabilities with ground-truth labels for DNIP optimization, except for AGNews, DBpedia, and DDI, for which we randomly select 10,000 training examples, since the datasets are quite large. We further split the training set into 95% optimization set and 5% development set. Test evaluations are performed on each test set against overall accuracy and COBias, except for AGNews, for which we evaluate on 5,000 randomly selected test examples.

E Performance Improvements vs. Number of Optimization Examples

We evaluate DNIP with varying optimization examples on Llama-2-13B. We find that DNIP requires only a small optimization set of 10 examples for a fair improvement in both COBias and accuracy, and it exhibits a further, emergent COBias reduction at several thousands optimization examples.

Test COBias reduction reaches 9% to 72% at 10 optimization examples, and continues to grow with more optimization examples. Figure 7 shows the relative test COBias reduction over ICL results. At 10 examples, DNIP can achieve a relative COBias reduction ranging from 9% to 72%. We observe an overall trend of COBias reduction except for DDI and PubMedQA, who have a spike at 100 examples, but DDI rises again after 500 examples while PubMedQA levels off (PubMedQA full

DNIP Objective (Results without DNIP are shown in the last row.)	Evaluation Metric									
	CB	CB _s	H	Overall Acc.	Class Acc.					
					Trbl.	Bad	Ok	Gd.	Grt.	
Z _{CB}	18.7	13.2	36.8	48.3	47.0	56.6	19.4	54.1	56.6	
Z _{CB_s}	29.3	22.5	38.6	49.3	50.7	59.3	0.9	68.9	54.4	
Z _H	35.6	34.8	34.8	50.6	37.2	70.9	0.9	68.8	53.3	
ICL	53.1	63.9	53.1	44.9	28.7	71.6	0.0	81.6	10.8	

Table 12: Comparison of SST-5 test set evaluation scores (%) for three DNIP objective functions Z_{CB} , Z_{CB_s} , and Z_H . Average scores over three runs of different 1-shot demonstrations are reported.

DNIP Objective (Results without DNIP are shown in the last row.)	Evaluation Metric									
	CB	CB _s	H	Overall Acc.	Class Acc.			Yes	No	Mayb.
					Yes	No	Mayb.			
Z _{CB}	41.1	31.3	38.9	63.1	74.4	61.1	12.7			
Z _{CB_s}	16.1	17.1	37.1	52.4	56.9	51.5	32.7			
Z _H	36.3	24.3	27.8	62.7	65.9	72.0	17.6			
ICL	61.2	65.0	44.0	55.1	42.2	93.7	1.8			

Table 13: Comparison of PubMedQA test set evaluation scores (%) for three DNIP objective functions Z_{CB} , Z_{CB_s} , and Z_H . Average scores over three runs of different 1-shot demonstrations are reported.

optimization size: 950). An explanation is that DNIP prioritizes COBias reduction more than accuracy increase at fewer examples; at more examples, the accuracy-related objectives show more influence. It also indicates that domain-specific datasets are more sensitive to the trade-off. We further notice a surge in reductions from 1,000 to full for DDI, SST-5, and DBpedia (full optimization sizes: 9,500, 8,116, 9,500), suggesting that around 8,000 examples are needed for a further emergent reduction - PubMedQA may see further COBias reduction if more optimization examples are available.

Test accuracy is improved with only 10 optimization examples, and plateaus at around 500 examples. Figure 8 shows that, at 10 examples, the relative increase in accuracy ranges from 0.2% to 11% except DDI, which is 160%. At 100 examples, the increase ranges from 3% to 208% (DDI, 7.2% \rightarrow 18.7%). The increase continues to grow and stabilizes at around 500 examples. At 1,000 examples, test accuracy for DDI rises to 52%, which is more than 6 times of the ICL accuracy, showing that DNIP is effective for this challenging biomedical NLP task.

Moreover, we observe for RTE a declining trend of accuracy increase, which matches its growing trend of COBias reduction, reflecting the trade-off between the two objectives. We also note a slight decrease in accuracy improvement for SST-5 and DDI at full size, which matches their sudden increase in COBias reduction, verifying that DNIP has emergent COBias reduction abilities with thousands of optimization examples. Overall, DNIP improves both accuracy and COBias at 10 examples, and achieves acceptable COBias reduction and accuracy improvement at 100 examples, with test COBias reduced by 57% and test accuracy improved. For detailed scores, please refer to Appendix I.

F Additional Heatmaps for Pairwise Accuracy Differences

Figure 9 and 10 demonstrate that more balanced class accuracies are achieved with DNIP for smaller LLMs of Llama-2-7B and GPT-2-XL.

G Additional Ablation Analysis

We show ablation analysis on GPT-2-XL and Llama-2-7B in Figure 11 and 12.

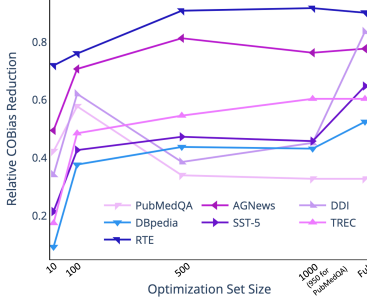


Figure 7: Relative test COBias reduction; higher is better.

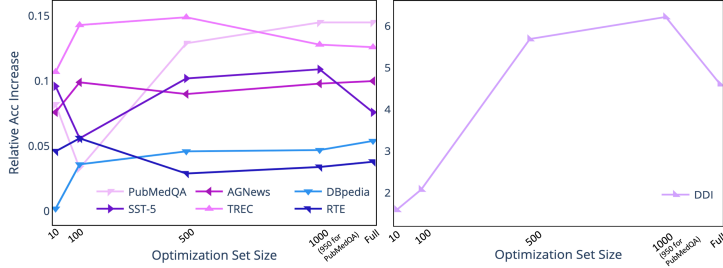


Figure 8: Relative test accuracy increase; higher is better.

H More Discussions

Optimization Algorithms for Integer Programming. The classic solvers for integer programming include operational research techniques such as Branch and Bound (BnB), commonly used for linear integer programming problems. However, it is difficult for these methods to solve our DNIP model, which contains discontinuous functions and is non-differentiable. In this case, a series of metaheuristic algorithms are more suitable, solvers including Simulated Annealing (SA), Genetic Algorithms, Ant Colony Optimization, and Particle Swarm Optimization. These algorithms all belong to the same category, and each meta heuristic has their own pros and cons. Therefore, SA in this paper has a clear purpose of tackling our NIP mathematical model that classical operational research methods cannot solve.

Our Motivation Is Different from Classical Post-hoc Corrections. Some may contend that achieving equitable accuracies across all classes is a well-explored issue in standard machine learning classifiers. However, it is crucial to see that class prediction accuracy imbalances must be understood within their specific context. The accuracy bias in LLMs' outputs arises from fundamentally different causes than the unequal class accuracies seen in potentially overfitted traditional classifiers. In the former, biases stem from prompts and pre-training, while in the latter, the imbalance is driven by skewness in the supervised training data. This distinction underscores why our approach is uniquely applied to LLMs' output token class probabilities.

Using Calibration Methods to Mitigate ICL Biases. Previous calibration methods reduce biases caused by prompting. For example, Zhao et al. [19], Zhou et al. [29] use content-free or content-based prompts to measure an offset and calibrate class probabilities by removing it. This may be good for mitigating bias towards a single class, but it does not consider the interaction between class predictions, e.g., pairwise class accuracy bias studied in this work. Another hazard is using prompts to compute the offset, which may cascade biases brought by a certain or several prompt templates, and biases inherited from pretraining may not be reflected. Instead, we correct biased predictions without more prompting, but we differ in that our correction weights are explicitly optimized on COBias and accuracy metrics, while the cluster-based decision boundary is implicitly learned.

Using Chain-of-Thought Prompting to Improve LLM Predictions. Some may argue that a simple remedy for biased predictions is Chain-of-Thought (CoT) prompting, which elicit more reasoning in

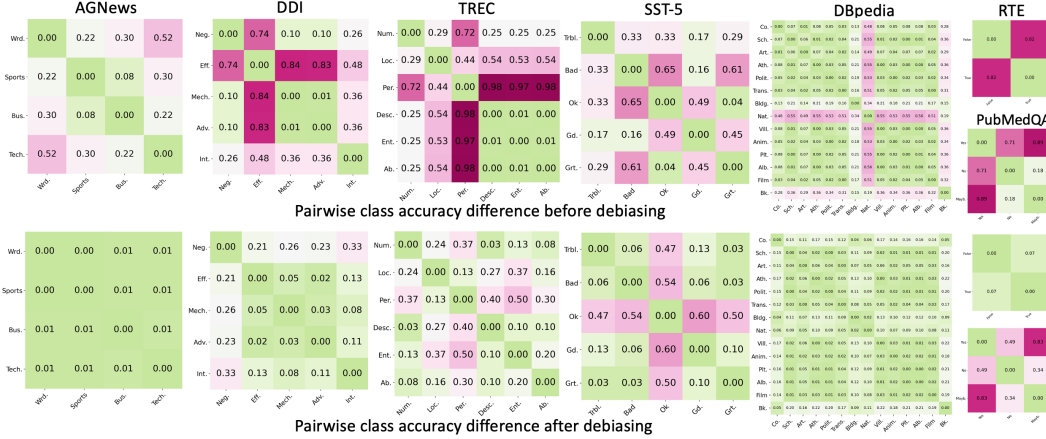


Figure 9: Comparisons of pairwise test class accuracy differences before and after applying DNIP on GPT-2-XL; the pinker the higher accuracy difference, the greener the lower accuracy difference; average accuracy over three runs are used.

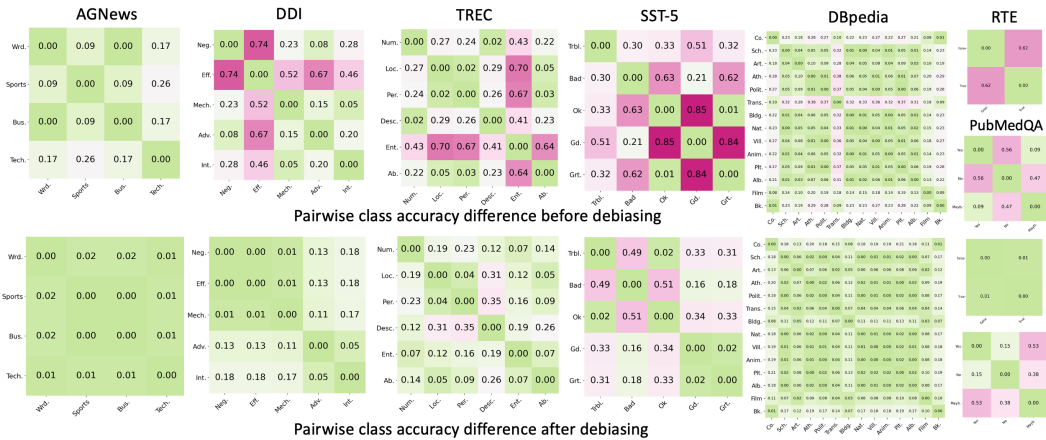


Figure 10: Comparisons of pairwise test class accuracy differences before and after applying DNIP on Llama-2-7B; the pinker the higher accuracy difference, the greener the lower accuracy difference; average accuracy over three runs are used.

LLMs. However, Turpin et al. [25] points out that CoT explanations can be unfaithful, as they can be biased towards class A when prompts always put letter A as the answer, causing 36% accuracy drops on BBH [32]. We add that prompt-based models may fall for pattern matching instead of recalling learned factual knowledge [20]. Therefore, CoT may not help due to unfaithful explanations.

I Full Table with Varying Number of Optimization Examples for DNIP

As an addition to Appendix E, the full results for all three models across varying optimization set sizes are shown in Table 14.

Opt. set	Eval. Metric	AGNews	DBpedia	SST-5	TREC	RTE	DDI	PubMedQA
<i>GPT-2-XL</i>								
0	Acc	52.1 _{5.4}	31.8 _{9.9}	34.9 _{13.7}	27.4 _{10.5}	55.4 _{1.9}	14.5 _{4.4}	55.2 _{0.0}
	COBias	35.5 _{11.5}	40.0 _{3.6}	48.7 _{5.4}	45.6 _{8.7}	82.4 _{24.5}	40.7 _{5.9}	59.4 _{12.6}
10*	Acc	72.8 _{2.1}	40.6 _{5.2}	40.3 _{3.4}	51.5 _{5.7}	50.3 _{0.8}	23.5 _{1.0}	53.7 _{0.6}
	COBias	17.2 _{1.7}	28.0 _{6.6}	40.1 _{1.8}	39.7 _{1.0}	6.5 _{7.6}	40.6 _{3.5}	41.8 _{0.0}
100	Acc	70.0 _{5.0}	41.4 _{29.9}	44.3 _{1.3}	49.0 _{10.1}	49.8 _{2.5}	42.2 _{5.7}	46.7 _{10.8}
	COBias	14.8 _{1.3}	27.8 _{8.9}	30.8 _{3.4}	31.1 _{5.9}	5.3 _{4.9}	17.1 _{7.1}	29.2 _{16.6}
500	Acc	68.2 _{1.2}	44.5 _{33.2}	43.4 _{1.5}	49.9 _{8.5}	50.5 _{2.4}	45.6 _{9.2}	49.9 _{11.4}
	COBias	2.7 _{1.8}	25.7 _{9.6}	29.8 _{3.7}	31.4 _{6.2}	5.2 _{3.9}	24.5 _{14.3}	17.7 _{15.8}
1,000	Acc	69.6 _{1.0}	42.0 _{32.2}	42.8 _{2.3}	50.9 _{9.0}	50.3 _{2.2}	48.3 _{4.9}	same as full
	COBias	3.0 _{1.2}	27.6 _{11.0}	28.2 _{5.9}	24.5 _{5.4}	5.2 _{3.3}	22.9 _{2.5}	
Full	Acc	68.5 _{1.0}	69.9 _{9.1}	44.5 _{2.20}	46.3 _{12.7}	50.8 _{2.1}	43.9 _{14.9}	57.1 _{1.3}
	COBias	1.4 _{0.5}	24.1 _{8.3}	26.0 _{2.5}	27.2 _{7.2}	7.1 _{5.0}	17.0 _{7.1}	29.8 _{25.0}
<i>Llama-2-7B</i>								
0	Acc	86.4 _{2.5}	88.9 _{2.0}	42.1 _{11.1}	66.7 _{6.6}	66.3 _{4.3}	6.7 _{0.4}	40.3 _{6.7}
	COBias	14.0 _{6.5}	13.5 _{2.1}	55.6 _{1.5}	33.2 _{10.0}	61.6 _{10.5}	41.4 _{1.7}	40.9 _{16.1}
10*	Acc	86.4 _{2.5}	89.9 _{1.4}	51.4 _{0.9}	70.1 _{0.9}	74.9 _{2.1}	31.7 _{21.0}	44.5 _{0.6}
	COBias	14.0 _{6.5}	12.5 _{2.1}	36.2 _{3.6}	22.4 _{5.4}	4.8 _{5.1}	26.7 _{8.2}	28.7 _{3.9}
100	Acc	88.4 _{0.4}	91.8 _{0.7}	50.9 _{1.5}	70.1 _{1.0}	73.6 _{2.6}	44.9 _{2.5}	62.6 _{4.5}
	COBias	5.8 _{0.6}	9.7 _{1.0}	34.3 _{12.7}	16.7 _{2.4}	2.9 _{0.7}	21.0 _{6.6}	35.4 _{18.1}
500	Acc	86.8 _{0.9}	92.1 _{0.6}	50.8 _{1.7}	69.7 _{1.2}	74.3 _{2.9}	69.3 _{1.7}	63.5 _{7.5}
	COBias	2.8 _{0.3}	8.6 _{1.6}	35.8 _{12.3}	15.2 _{2.1}	3.1 _{1.4}	34.5 _{0.3}	37.3 _{20.4}
1,000	Acc	86.8 _{0.3}	92.5 _{0.2}	51.0 _{2.1}	69.5 _{0.8}	74.0 _{2.5}	56.5 _{7.9}	same as full
	COBias	1.9 _{0.5}	8.0 _{0.4}	30.9 _{20.4}	15.7 _{1.2}	2.6 _{1.2}	29.5 _{3.4}	
Full	Acc	86.7 _{0.4}	92.9 _{0.4}	50.6 _{2.7}	68.1 _{1.0}	73.9 _{2.3}	44.5 _{3.8}	62.7 _{8.3}
	COBias	1.3 _{0.1}	7.7 _{0.6}	28.0 _{21.6}	15.9 _{1.6}	1.9 _{1.8}	11.6 _{3.0}	35.4 _{22.8}
<i>Llama-2-13B</i>								
0	Acc	79.9 _{7.0}	88.6 _{1.7}	44.9 _{4.3}	68.5 _{10.8}	71.5 _{2.2}	7.2 _{0.9}	55.1 _{2.9}
	COBias	28.3 _{16.1}	16.2 _{3.7}	53.1 _{5.0}	35.9 _{6.5}	43.4 _{7.0}	45.6 _{5.9}	61.2 _{1.9}
10*	Acc	86.0 _{1.9} /	88.8 _{1.6} /	49.2 _{0.8} /	75.8 _{3.2}	74.8 _{2.3}	18.7 _{12.6}	59.6 _{6.2}
	COBias	14.3 _{3.5}	14.7 _{2.5}	41.7 _{8.1}	29.6 _{4.5}	12.2 _{5.7}	30.0 _{7.8}	35.3 _{7.8}
100	Acc	87.8 _{0.2} /	91.8 _{0.2} /	47.4 _{2.0} /	78.3 _{2.8}	75.5 _{1.0}	22.2 _{2.0}	56.9 _{10.4}
	COBias	8.3 _{0.5}	10.1 _{0.7}	30.4 _{4.4}	18.5 _{2.6}	10.4 _{6.9}	17.3 _{4.4}	25.8 _{16.3}
500	Acc	87.1 _{1.5}	92.7 _{0.0} /	49.5 _{0.7} /	78.7 _{2.1}	73.6 _{1.7}	48.2 _{27.4}	62.2 _{15.8}
	COBias	5.3 _{3.1}	9.1 _{0.3}	28.0 _{3.2}	16.3 _{1.0}	4.0 _{3.4}	28.0 _{11.5}	40.4 _{29.4}
1,000	Acc	87.7 _{0.7} /	92.8 _{0.1} /	49.8 _{0.7} /	77.3 _{2.0}	73.9 _{1.5}	52.0 _{10.5}	same as full
	COBias	6.7 _{1.5}	9.2 _{0.2}	28.8 _{2.0}	14.2 _{1.8}	3.6 _{4.3}	25.0 _{9.7}	
Full	Acc	87.9 _{0.7}	93.4 _{0.6}	48.3 _{1.9}	77.1 _{2.0}	74.3 _{0.8}	40.4 _{6.0}	63.1 _{14.0}
	COBias	6.3 _{0.6}	7.7 _{0.6}	18.7 _{10.1}	14.2 _{1.3}	4.3 _{3.3}	7.5 _{3.2}	41.1 _{29.6}

Table 14: Comparisons of DNIP results on varying optimization set sizes; min. optimization set size is 10 for all datasets except for DBpedia, which we use 15 to cover its 14 classes. For full optimization set sizes, AGNews: 9,500, DBpedia: 9,500, SST-5: 8,116, TREC: 5,179, RTE: 2,365, DDI: 9,500, PubMedQA: 950.

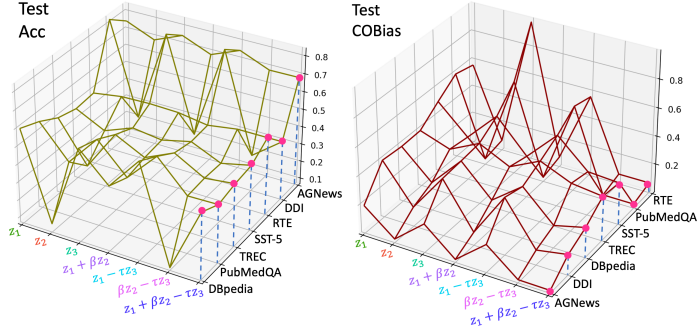


Figure 11: Ablations on objective function, GPT-2-XL, demonstrating that $z_1 + \beta z_2 - \tau z_3$ achieves a balance point between accuracy and COBias.

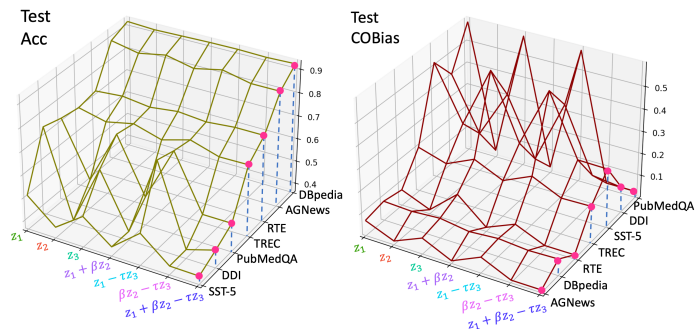


Figure 12: Ablations on objective function, Llama-2-7B, demonstrating that $z_1 + \beta z_2 - \tau z_3$ achieves a balance point between accuracy and COBias.